# J|A|C|S

JOURNAL OF THE AMERICAN CHEMICAL SOCIETY

Coassembly of Peptides Derived from β-Sheet Regions of β-Amyloid

Nicholas L. Truex and James S. Nowick*

Department of Chemistry, University of California, Irvine, Irvine, California 92697-2025, United States

S *Supporting Information*

ABSTRACT: In this paper, we investigate the coassembly of peptides derived from the central and C-terminal regions of the β-amyloid peptide (Aβ). In the preceding paper, *J. Am. Chem. Soc.* **2016**, DOI: 10.1021/jacs.6b06000, we established that peptides containing residues 17−23 (LVFFAED) from the central region of Aβ and residues 30−36 (AIIGLMV) from the C-terminal region of Aβ assemble to form homotetramers consisting of two hydrogen-bonded dimers. Here, we mix these tetramer-forming peptides and determine how they coassemble. Incorporation of a single ^{15}N isotopic label into each peptide provides a spectroscopic probe with which to elucidate the coassembly of the peptides by $^1H,^{15}N$ HSQC. Job's method of continuous variation and nonlinear least-squares fitting reveal that the peptides form a mixture of heterotetramers in 3:1, 2:2, and 1:3 stoichiometries, in addition to the homotetramers. These studies also establish the relative stability of each tetramer and show that the 2:2 heterotetramer predominates. ^{15}N-Edited NOESY shows the 2:2 heterotetramer comprises two different homodimers, rather than two heterodimers. The peptides within the heterotetramer segregate in forming the homodimer subunits, but the two homodimers coassemble in forming the heterotetramer. These studies show that the central and C-terminal regions of Aβ can preferentially segregate within β-sheets and that the resulting segregated β-sheets can further coassemble.
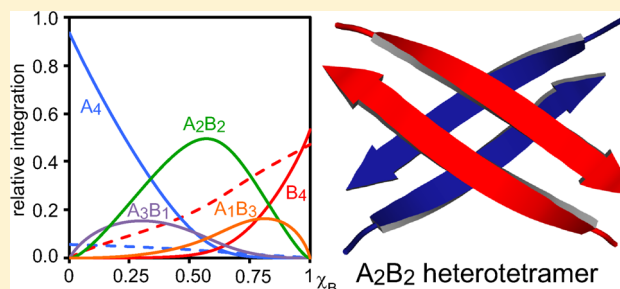
INTRODUCTION

Interactions among β-sheets are critical in the aggregation of the β-amyloid peptide (Aβ) to form oligomers and fibrils in Alzheimer's disease.[1] Two regions of the 40- or 42-residue peptide adopt β-sheet structure and promote aggregation: the central region and the C-terminal region.[2] The central region comprises the hydrophobic pentapeptide LVFFA (Aβ$_{17−23}$), and the C-terminal region comprises the hydrophobic undecapeptide AIIGLMVGGVV (Aβ$_{30−40}$) or the hydrophobic tridecapeptide AIIGLMVGGVVIA (Aβ$_{30−42}$).

Elucidating the roles of the central and C-terminal regions of Aβ is critical to understanding Aβ aggregation. These two regions assemble differently in the fibrils and in the toxic oligomers that cause synaptic dysfunction and cell death. In Aβ$_{1−40}$ fibrils, the peptide forms parallel β-sheets, with the central and C-terminal regions laminated together.[3,4] In the oligomers, the peptide is thought to form β-hairpins comprising antiparallel β-sheets.[5]

In the preceding paper,[6] we incorporated residues from the central and C-terminal regions into macrocyclic β-sheet peptides **1**, and we determined how the peptides assembled in aqueous solution.[6] Peptides **1** consist of a heptapeptide strand, a template strand containing the unnatural amino acid Hao, and two δ-linked ornithine turn units.[7−9] We incorporated residues LVFFAED (Aβ$_{17−23}$) and residues AIIGLMV (Aβ$_{30−36}$) into the heptapeptide strands of peptides **1a** and **1b**, respectively. We incorporated isoleucine residues (I$_8$ and I$_{11}$) into the template strand to promote assembly and lysine residues (K$_9$ and K$_{10}$) to maintain solubility. ^1H NMR studies of peptides **1a** and **1b** show

that the peptides assemble to form sandwich-like homotetramers, consisting of two hydrogen-bonded dimers.
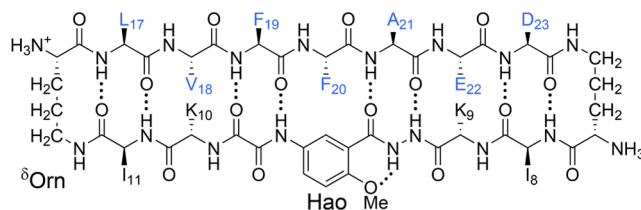
macrocyclic β-sheet peptide **1a**
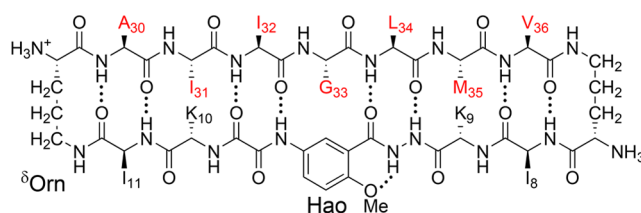
macrocyclic β-sheet peptide **1b**

Incorporation of a single isotopic label into peptides **1** facilitated the identification and quantification of the tetramers. The peptides [^{15}N]**1a** and [^{15}N]**1b** each contain a single ^{15}N-labeled amino acid in the center of the heptapeptide strand. Peptide [^{15}N]**1a** contains an ^{15}N label in the F$_{20}$ residue; peptide
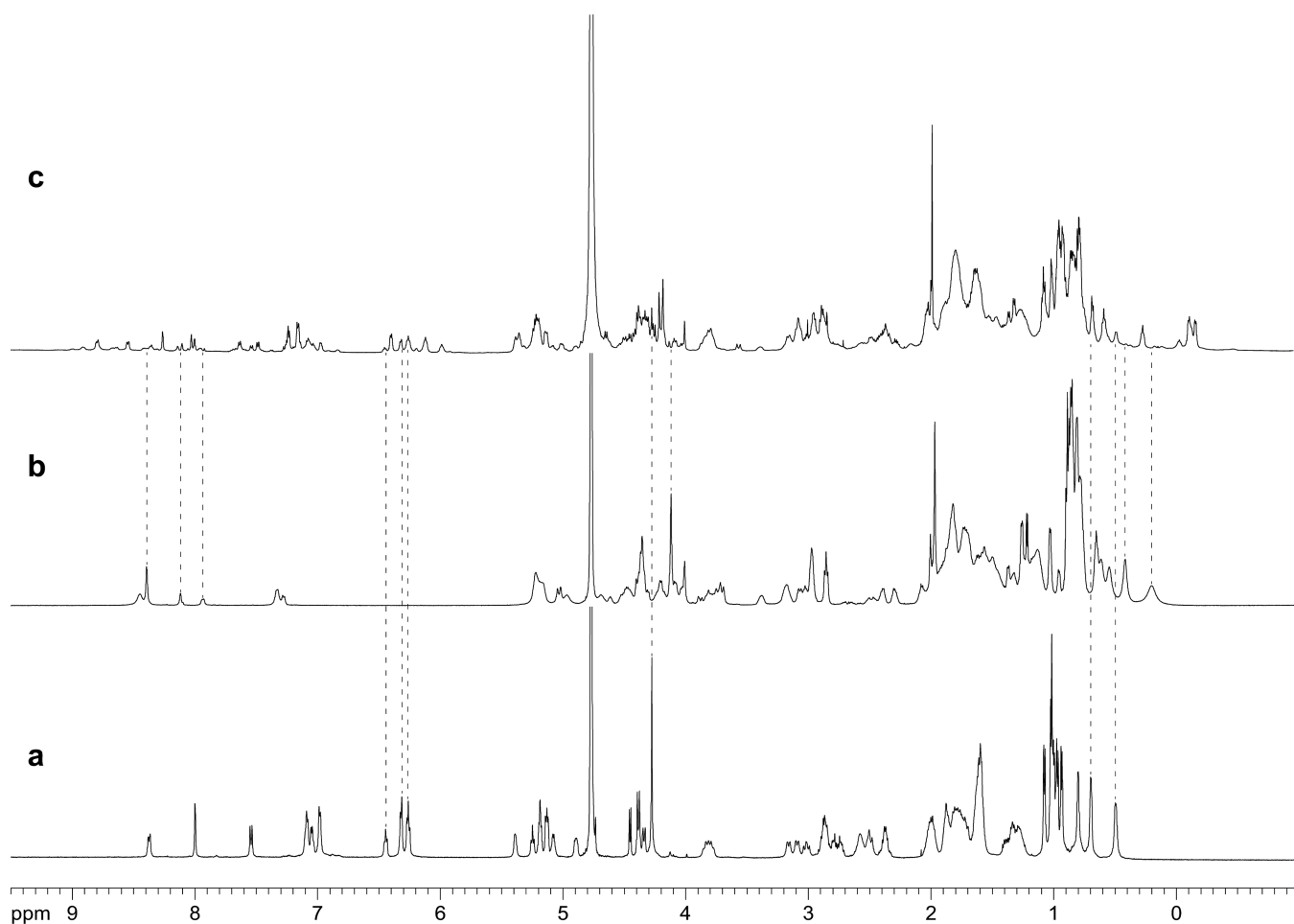
Figure 1. ^{1}H NMR spectra of (a) peptide **1a** at 8.0 mM, (b) peptide **1b** at 8.0 mM, and (c) the 1:1 mixture of peptides **1a** and **1b** at 8.0 mM total concentration in D$_2$O at 600 MHz and 298 K. Dotted lines illustrate how the resonances from the 1:1 mixture compare with the resonances of pure **1a** and pure **1b**.

[^{15}N]**1b** contains an ^{15}N label in the G$_{33}$ residue. ^{1}H,^{15}N HSQC studies show only the resonances associated with the ^{15}N label, reducing each spectrum to two crosspeaks: The ^{1}H,^{15}N HSQC spectrum of peptide [^{15}N]**1a** shows one crosspeak associated with the monomer and another associated with the homotetramer. The ^{1}H,^{15}N HSQC spectrum of peptide [^{15}N]**1b** also shows one crosspeak associated with the monomer and another associated with the homotetramer.

In this paper, we ask whether these peptides prefer to coassemble or to segregate.[10] To address this question, we mix peptides **1a** and **1b** and characterize the oligomers that form. ^{1}H NMR studies show that peptides **1a** and **1b** form a mixture of homotetramers and heterotetramers, but the ^{1}H NMR spectrum of the mixture is largely indecipherable. To characterize the complex mixture of homotetramers and heterotetramers, we use the ^{15}N-labeled peptides [^{15}N]**1a** and [^{15}N]**1b** and ^{1}H,^{15}N NMR spectroscopy. ^{1}H,^{15}N HSQC, in conjunction with Job's method of continuous variation, reveals that the peptides form three heterotetramers in 3:1, 2:2, and 1:3 stoichiometries, in addition to the two homotetramers. The following describes the characterization of these five tetramers and the equilibria among them.

■ RESULTS AND DISCUSSION

Peptides 1a and 1b Coassemble upon Mixing. The ^{1}H NMR spectrum of pure peptide **1a** at 8.0 mM predominately

shows the homotetramer; the ^{1}H NMR spectrum of pure peptide **1b** at 8.0 mM shows the monomer and the homotetramer. In a 1:1 mixture of peptides **1a** and **1b** at 8.0 mM total concentration, the ^{1}H NMR spectrum shows many new resonances: The resonances from the homotetramer of peptide **1a** diminish greatly and the resonances from the homotetramer of peptide **1b** nearly disappear. New resonances appear in the spectrum in the aromatic region between 6 and 9 ppm and also in the methyl region below 1 ppm. Several new Hao methoxy (Hao$_{OMe}$) resonances appear between 4 and 4.5 ppm. The Hao$_{OMe}$ resonance from the homotetramer of peptide **1a** diminishes greatly and the Hao$_{OMe}$ resonance from the homotetramer of peptide **1b** almost completely disappears. The multitude of new resonances in the spectrum of the 1:1 mixture suggests that several new oligomers form, rather than just one. Figure 1 shows the ^{1}H NMR spectra of pure **1a**, pure **1b**, and the 1:1 mixture.

Peptides 1a and 1b Form Heterotetramers. We have previously shown that related macrocyclic β-sheets can assemble to form tetramers.[11] In the preceding paper,[6] we established that both peptide **1a** and peptide **1b** form tetramers by measuring the diffusion coefficients (D) with DOSY NMR.[6] Here, we use DOSY NMR to determine whether the species that form upon mixing peptides **1a** and **1b** are also tetramers. The homotetramers of peptides **1a** and **1b** have diffusion coefficients of about 12×10^{-11} m^2/s in D$_2$O at 298 K. The diffusion

coefficients of the species that predominate in the 1:1 mixture are comparable, 11.4×10^{-11} m^2/s (Table 1), indicating that these species are also tetramers.

Table 1. Diffusion Coefficients (D) of Peptides 1a and 1b in D$_2$O at 298 K

	MW$_{tetramer}$[a] (Da)	conc (mM)	D ($\times 10^{-11}$ m^2/s)	oligomer state
1a	7068	8.0	11.8 ± 1.0	A$_4$ homotetramer
1b	6572	16.0	11.9 ± 1.1	B$_4$ homotetramer
1a + 1b		8.0[b]	11.4 ± 1.1	heterotetramers

[a]Molecular weight calculated for the neutral (uncharged) peptide. [b]Total concentration of the 1:1 mixture of peptides **1a** and **1b**.

In this paper, we describe the homotetramers and heterotetramers formed by peptides **1a** and **1b** using the letters A and B. The homotetramers are designated A$_4$ and B$_4$, and the 3:1, 2:2, and 1:3 heterotetramers are designated A$_3$B$_1$, A$_2$B$_2$, and A$_1$B$_3$. Two topological isomers of the A$_2$B$_2$ heterotetramer could form: one consisting of two homodimers (A·A and B·B); the other consisting of two heterodimers (A·B and A·B). Figure 2 illustrates the homotetramers and heterotetramers, where a single β-strand represents either peptide **1a** or **1b**.

The complex mixture of monomers, homotetramers, and heterotetramers can give as many as 16 resonances in the ^{1}H NMR spectrum: two from the A monomer and A$_4$ homotetramer; two from the B monomer and B$_4$ homotetramer, four from the A$_3$B$_1$ heterotetramer, four from the A$_1$B$_3$
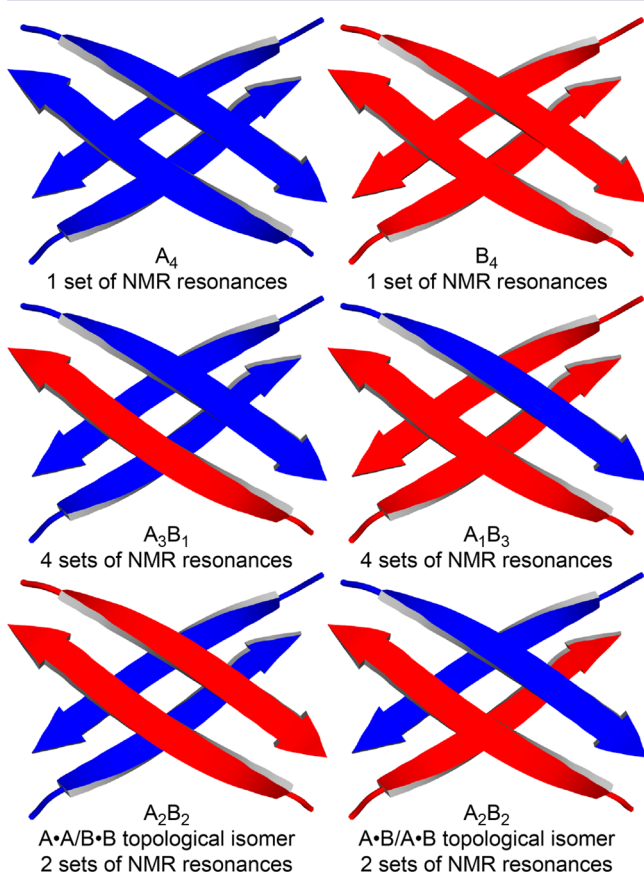

Figure 2. Cartoons illustrating homotetramers and heterotetramers, in which peptide **1a** is represented by a blue arrow and peptide **1b** is represented by a red arrow.

heterotetramer, and either two or four from the A$_2$B$_2$ heterotetramer. The A$_2$B$_2$ heterotetramer would give four resonances if both the A·A/B·B and A·B/A·B topological isomers formed, but only two resonances if just one of the two isomers formed.

Elucidation of the A$_2$B$_2$ Topological Isomer. We used peptides [^{15}N]**1a** and [^{15}N]**1b** to elucidate the dimers within the A$_2$B$_2$ heterotetramer. In the preceding paper,[6] we used these peptides and ^{15}N-edited NOESY to help establish the pairing of the dimers within the A$_4$ and B$_4$ homotetramers.[6] Here, we compare the ^{15}N-edited NOESY spectra of pure [^{15}N]**1a** and pure [^{15}N]**1b** to that of the 1:1 mixture to determine which A$_2$B$_2$ topological isomer forms (Figure 3). The spectra show that the A$_2$B$_2$ heterotetramer consists of an A·A and a B·B homodimer, and not of two A·B heterodimers (Figure 4).
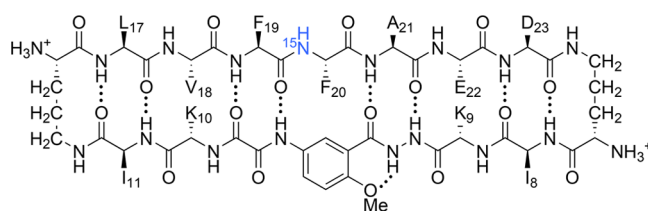
macrocyclic β-sheet peptide [^{15}N]**1a**
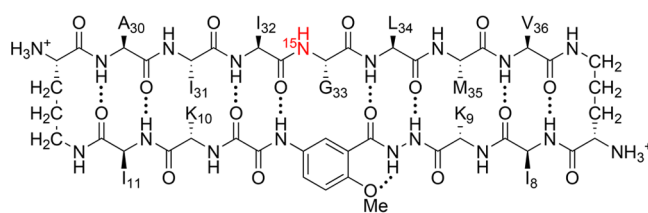
macrocyclic β-sheet peptide [^{15}N]**1b**

The ^{15}N-edited NOESY spectrum of the 1:1 mixture of peptides [^{15}N]**1a** and [^{15}N]**1b** shows four distinct sets of resonances: two sets associated with the A$_2$B$_2$ heterotetramer; one set associated with the A$_4$ homotetramer; and one set associated with the B monomer (Figure 3c). In addition to the NOEs, the spectrum also shows crosspeaks associated with chemical exchange between the monomer of peptide [^{15}N]**1b** and the A$_2$B$_2$ heterotetramer.

The A$_2$B$_2$ heterotetramer gives two sets of resonances: one set from the F$_{20}$NH proton of peptide [^{15}N]**1a** and the other set from the G$_{33}$NH proton of peptide [^{15}N]**1b**. The F$_{20}$NH proton of peptide [^{15}N]**1a** gives a strong interresidue NOE to the F$_{19}$Hα proton and a weaker intraresidue NOE to the F$_{20}$Hα proton. Figure 4a summarizes these NOEs. An intermolecular NOE between the F$_{20}$NH and the A$_{21}$Hα protons is not observed as a separate crosspeak because the F$_{20}$Hα and the A$_{21}$Hα resonances overlap.[12] The F$_{20}$NH proton gives an additional NOE to the A$_{21}$Hβ protons, which corroborates the proximity of these residues (Figure S2). An intermolecular NOE is not observed between the F$_{20}$NH proton of peptide [^{15}N]**1a** and the L$_{34}$Hα proton of peptide [^{15}N]**1b** (Figure 3c); an intermolecular NOE is also not observed between the F$_{20}$NH proton of peptide [^{15}N]**1a** and the G$_{33}$NH proton of peptide [^{15}N]**1b** (Figure S3). The absence of these two NOEs indicates that peptide [^{15}N]**1a** is not part of an A·B heterodimer (Figure 4c).

The G$_{33}$NH proton of peptide [^{15}N]**1b** gives an interresidue NOE to the I$_{32}$Hα proton and intraresidue NOEs to the G$_{33}$Hα and G$_{33}$Hα′ protons (Figure 3c). The G$_{33}$NH proton also gives
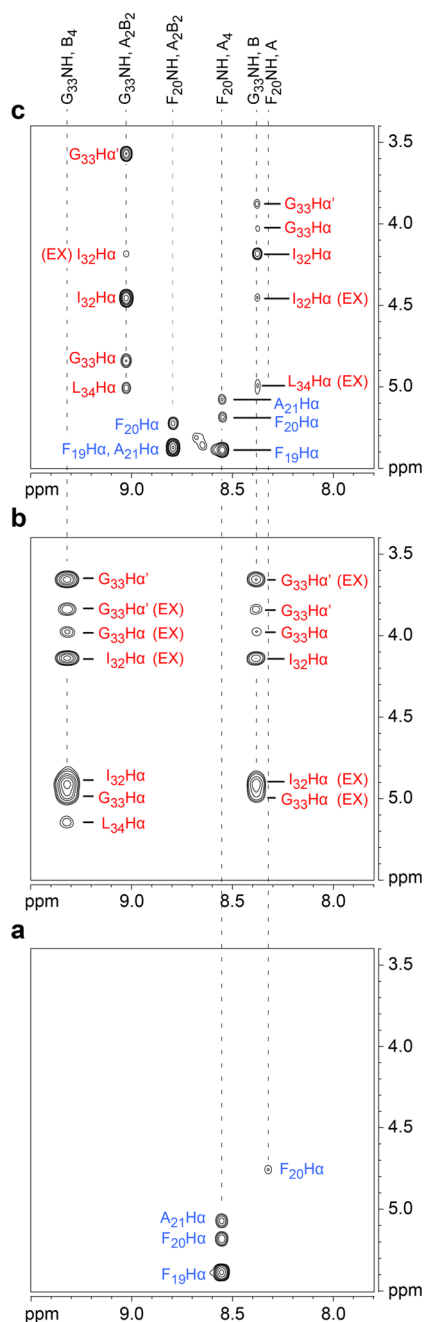
Figure 3. ^{15}N-Edited NOESY spectra of (a) peptide $[^{15}\text{N}]\mathbf{1a}$ at 8.0 mM, (b) peptide $[^{15}\text{N}]\mathbf{1b}$ at 8.0 mM, and (c) the 1:1 mixture of peptides $[^{15}\text{N}]\mathbf{1a}$ and $[^{15}\text{N}]\mathbf{1b}$ at 8.0 mM total concentration in 9:1 H_2O/D_2O at 600 MHz and 293 K. The $G_{33}H\alpha$ corresponds to the *pro-R* α-proton and the $G_{33}H\alpha'$ corresponds to the *pro-S* α-proton. Crosspeaks associated with chemical exchange of peptide **1b** between the monomer and the B_4 and A_2B_2 tetramers are labeled EX. Dotted lines illustrate how the crosspeaks from the 1:1 mixture compare with the crosspeaks of pure $[^{15}\text{N}]\mathbf{1a}$ and pure $[^{15}\text{N}]\mathbf{1b}$.
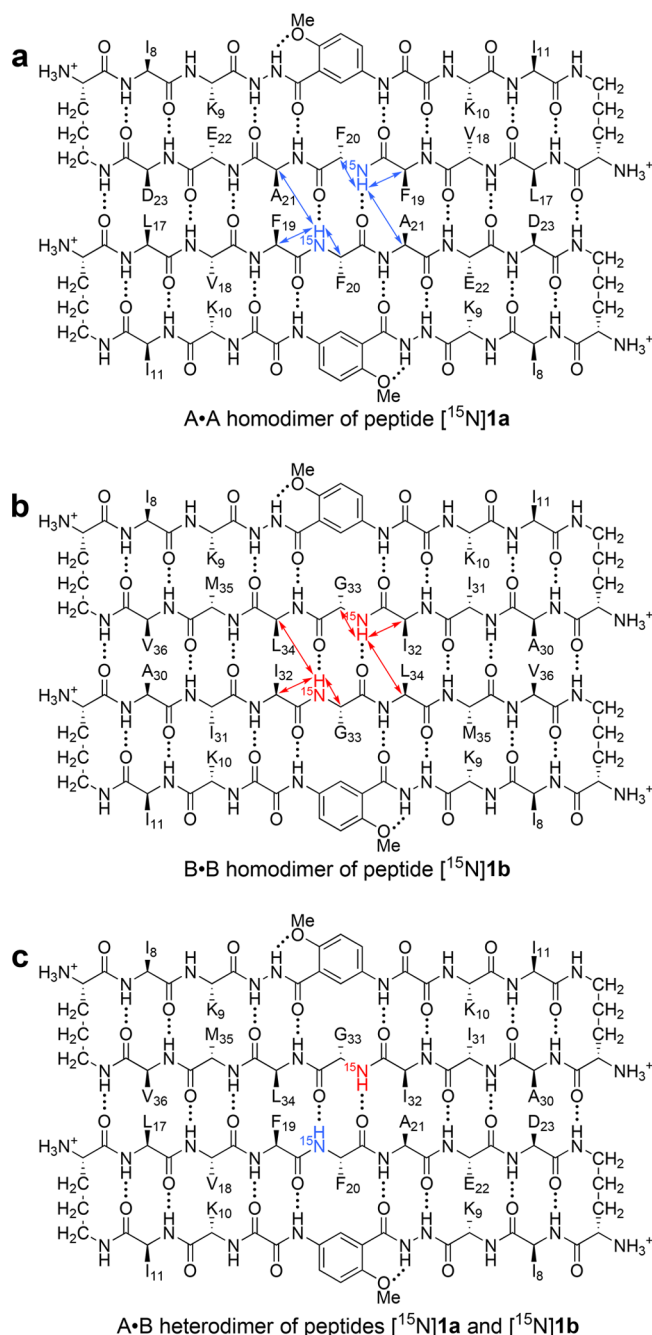

Figure 4. NOEs involving the ^{15}NH protons within the A_2B_2 heterotetramer. (a) The A·A homodimer with blue arrows illustrating the NOEs observed within the dimers. (b) The B·B homodimer with red arrows illustrating the NOEs observed within the dimers. (c) The A·B heterodimer (not formed).

an intermolecular NOE to the $L_{34}H\alpha$ proton.[12] This NOE confirms that the B·B homodimer forms within the A_2B_2 heterotetramer and rules out the A·B heterodimer. Figure 4b summarizes these NOEs.[13] Collectively, the ^{15}N-edited NOESY studies establish that the A·A/B·B topological isomer that forms exclusively is the A_2B_2 heterotetramer.

^{1}H,^{15}N HSQC Reveals That Peptides $[^{15}\text{N}]\mathbf{1a}$ and $[^{15}\text{N}]\mathbf{1b}$ Form Three Heterotetramers: A_3B_1, A_2B_2, and A_1B_3.

We compared the ^{1}H,^{15}N HSQC spectra of pure $[^{15}\text{N}]\mathbf{1a}$ and pure $[^{15}\text{N}]\mathbf{1b}$ to that of the 1:1 mixture to show which crosspeaks are associated with heterotetramers.[6] The ^{1}H,^{15}N HSQC spectrum of the 1:1 mixture of peptides $[^{15}\text{N}]\mathbf{1a}$ and $[^{15}\text{N}]\mathbf{1b}$ at 8.0 mM total concentration shows 10 new crosspeaks (14 crosspeaks in total). The crosspeaks are sharp and distinct, indicating that the tetramers exchange slowly on the NMR time scale. The two crosspeaks designated 1 and 2 come from the monomer and homotetramer of peptide $[^{15}\text{N}]\mathbf{1a}$; the two crosspeaks designated 3 and 4 come from the monomer and homotetramer of peptide $[^{15}\text{N}]\mathbf{1b}$. The 10

remaining crosspeaks designated 5−14 come from the heterotetramers. Figure 5a shows the ^{1}H,^{15}N HSQC spectrum of the 1:1 mixture of peptides [^{15}N]1a and [^{15}N]1b. Table 2 summarizes the chemical shifts of crosspeaks 1−14.
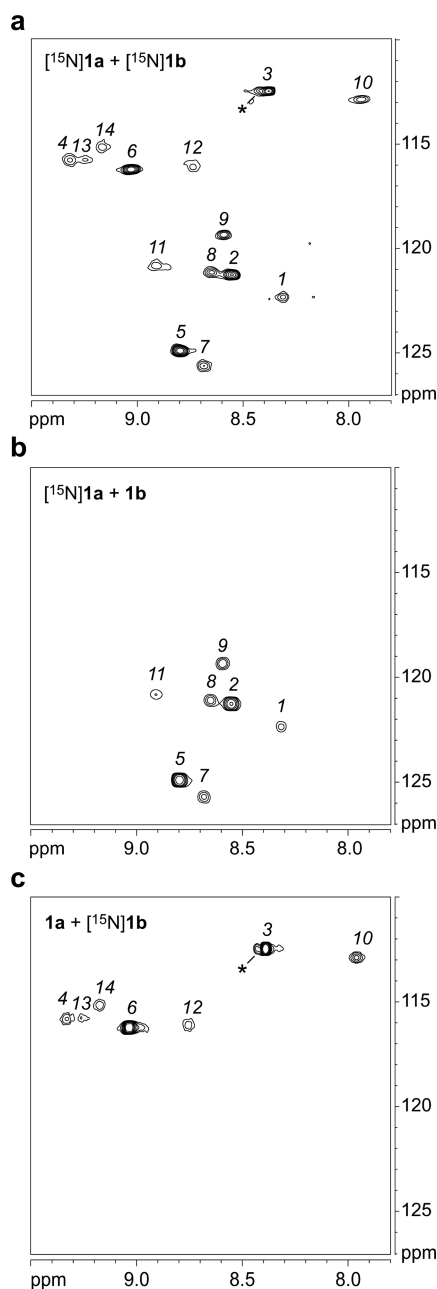
Figure 5. ^{1}H,^{15}N HSQC spectra of 8.0 mM mixtures in 9:1 H$_2$O/D$_2$O at 600 MHz and 293 K of peptides: (a) [^{15}N]1a and [^{15}N]1b; (b) [^{15}N] 1a and 1b; (c) 1a and [^{15}N]1b. The asterisk (*) indicates a crosspeak from a minor unidentified species associated with peptide [^{15}N]1b.

The remaining crosspeaks 5−14 come from the A$_3$B$_1$, A$_2$B$_2$, and A$_1$B$_3$ heterotetramers. Crosspeaks 5 and 6 are prominent and strikingly similar in intensity to each other. These two crosspeaks come from the A$_2$B$_2$ heterotetramer. Crosspeaks 7−14 are weaker and are also similar in intensity to each other. These eight crosspeaks are associated with the A$_3$B$_1$ and A$_1$B$_3$ heterotetramers.

We mixed peptides [^{15}N]1a and 1b and also mixed peptides 1a and [^{15}N]1b to assign crosspeaks 7−14 to the respective

Table 2. Chemical Shifts of Peptides [^{15}N]1a and [^{15}N]1b

crosspeak	δ F$_{20}$		δ G$_{33}$		species
	^{1}H	^{15}N	^{1}H	^{15}N	
1	8.32	122.3			A monomer
2	8.56	121.3			A$_4$ homotetramer
3			8.39	112.5	B monomer
4			9.33	115.8	B$_4$ homotetramer
5	8.81	124.9			A$_2$B$_2$ heterotetramer
6			9.03	116.2	A$_2$B$_2$ heterotetramer
7	8.69	125.7			A$_3$B$_1$ heterotetramer
8	8.66	121.1			A$_3$B$_1$ heterotetramer
9	8.60	119.3			A$_3$B$_1$ heterotetramer
10			7.94	112.8	A$_3$B$_1$ heterotetramer
11	8.92	120.9			A$_1$B$_3$ heterotetramer
12			8.74	116.1	A$_1$B$_3$ heterotetramer
13			9.25	115.8	A$_1$B$_3$ heterotetramer
14			9.17	115.1	A$_1$B$_3$ heterotetramer

^{a}^{1}H,^{15}N HSQC spectrum was recorded for the 1:1 mixture at 8.0 mM in 9:1 H$_2$O/D$_2$O at 293 K.

peptides. Figure 5b,c shows the ^{1}H,^{15}N HSQC spectra of these mixtures of labeled and unlabeled peptides. The ^{1}H,^{15}N HSQC spectrum of peptides [^{15}N]1a and 1b shows that crosspeaks 1, 2, 5, 7, 8, 9, and 11 come from peptide [^{15}N]1a; the ^{1}H,^{15}N HSQC spectrum of peptides 1a and [^{15}N]1b shows that crosspeaks 3, 4, 6, 10, 12, 13, and 14 come from peptide [^{15}N]1b. These spectra confirm that half of the crosspeaks come from peptide 1a and that half of the crosspeaks come from peptide 1b.

Assigning the ^{1}H,^{15}N HSQC Crosspeaks of the A$_3$B$_1$ and A$_1$B$_3$ Heterotetramers. To assign which of the crosspeaks 7−14 come from the A$_3$B$_1$ heterotetramer and which come from the A$_1$B$_3$ heterotetramer, we compared ^{1}H,^{15}N HSQC spectra of 3:1 and 1:3 mixtures of peptides [^{15}N]1a and [^{15}N]1b to that of the 1:1 mixture. In the spectra of the 3:1, 1:1, and 1:3 mixtures, the relative intensities of crosspeaks 1−14 vary, but the chemical shifts do not. The f_1 projections of the ^{1}H,^{15}N HSQC spectra conveniently illustrate the relative intensities of the crosspeaks as one-dimensional ^{15}N spectra. Figure 6 shows the f_1 projections of pure [^{15}N]1a, the 3:1, 1:1, and 1:3 mixtures, and pure [^{15}N]1b.

The systematic variation of the crosspeaks as a function of the mole fraction χ_B clearly establishes which crosspeaks are associated with the A$_3$B$_1$ heterotetramer and which are associated with the A$_1$B$_3$ heterotetramer. Crosspeaks 7−10 have maximum relative intensities at $\chi_B = 0.25$ and come from the A$_3$B$_1$ heterotetramer. Crosspeaks 11−14 have maximum relative intensities at $\chi_B = 0.75$ and come from the A$_1$B$_3$ heterotetramer. Figure 7 illustrates relative integrations of the crosspeaks versus the mole fraction of peptide [^{15}N]1b, χ_B.

Job's Method of Continuous Variation. We used Job's method to determine the relative stabilities of the homotetramers and the heterotetramers of peptides [^{15}N]1a and [^{15}N] 1b. Although this method was first introduced to study inorganic complexes, it is useful in all areas of chemistry for studying molecular association.[14,15] Job's method is performed by mixing two compounds "A" and "B" in varying ratios while keeping the total concentration constant. The amount of a complex that forms is then plotted versus the mole fraction to give a plot known as a "Job plot". The appearance of the Job plot reflects the stoichiometry and relative stability of each complex. The mole fraction at which the maximum amount of the complex forms corresponds with its stoichiometry. For example,
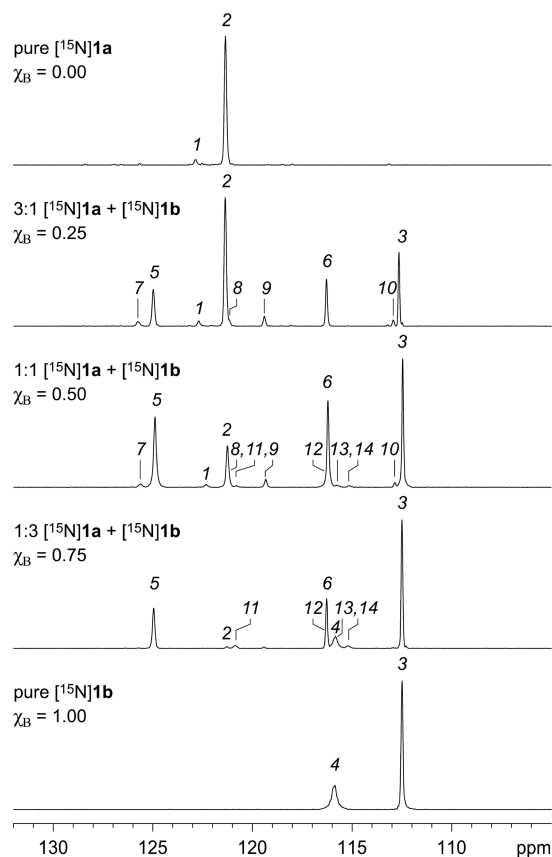
Figure 6. ^{15}N spectra from the f_1 projections of the $^1H,^{15}N$ HSQC spectra of mixtures of peptides $[^{15}N]\mathbf{1a}$ and $[^{15}N]\mathbf{1b}$. Spectra were recorded at 8.0 mM total concentration and varying mole fractions of peptide in 9:1 H_2O/D_2O at 600 MHz and 293 K. The mole fraction of peptide $[^{15}N]\mathbf{1b}$ is designated χ_B.
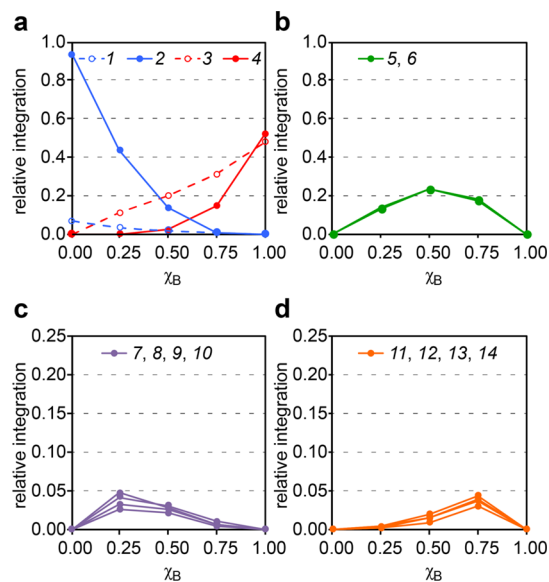

Figure 7. Plot of the relative integrations of crosspeaks 1−14 versus the mole fraction of peptide $[^{15}N]\mathbf{1b}$, χ_B. The intensities were measured by integrating the crosspeaks in the $^1H,^{15}N$ HSQC spectra of the mixtures of peptides $[^{15}N]\mathbf{1a}$ and $[^{15}N]\mathbf{1b}$.

an A_1B_2 heterotrimer would give a maximum in a 1:2 mixture ($\chi_B = 0.67$).

We applied Job's method to peptides $[^{15}N]\mathbf{1a}$ and $[^{15}N]\mathbf{1b}$, recording $^1H,^{15}N$ HSQC spectra for nine samples at 8.0 mM total concentration.[16] We plotted the sum of the relative integrals of the $^1H,^{15}N$ HSQC crosspeaks for each species versus the mole fraction of peptide $[^{15}N]\mathbf{1b}$, χ_B. For example, we plotted the curve for the A_3B_1 heterotetramer species using the sum of the relative integrals of crosspeaks 7−10. Figure 8 illustrates the resulting Job plot.
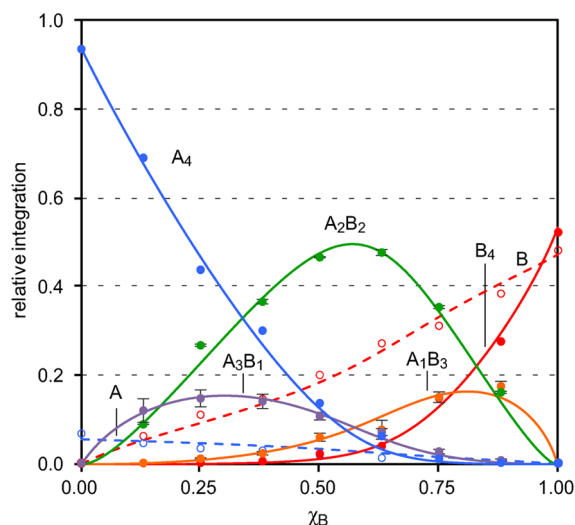

Figure 8. Job plot for peptides $[^{15}N]\mathbf{1a}$ and $[^{15}N]\mathbf{1b}$ showing the relative integrations of the monomers, homotetramers, and heterotetramers versus the mole fraction of peptide $[^{15}N]\mathbf{1b}$, χ_B. The curves reflect a monomer−tetramer equilibrium model fitted to the data. The error bars reflect the standard deviations among the individual measurements used to determine the relative integrations of A_3B_1, A_2B_2, and A_1B_3. The relative stabilities determined for each species are $\phi_{4,4} = 1.00$, $\phi_{4,3} = 0.22$, $\phi_{4,2} = 0.67$, $\phi_{4,1} = 0.12$, $\phi_{4,0} = 0.12$, $\phi_{1,1} = 0.36$, and $\phi_{1,0} = 2.20$.

The Job plot shows that the A_2B_2 heterotetramer predominates over a wide range of mole fractions. At low mole fractions, $\chi_B \leq 0.25$, the A_4 homotetramer predominates. At high mole fractions, $\chi_B \geq 0.75$, the B monomer and B_4 heterotetramer predominate. The A_2B_2 heterotetramer reaches a maximum concentration at a mole fraction χ_B slightly greater than 0.50. The A_3B_1 heterotetramer and the A_1B_3 heterotetramer form to a lesser extent, reaching a maximum concentration at low and high mole fractions χ_B, respectively.

Simulated Job Plots of Homotetramers and Heterotetramers. We generated simulated Job plots reflecting different homotetramer and heterotetramer stabilities to help interpret the data in Figure 8. We used an implementation developed by Collum and co-workers that readily accommodates homotetramer and heterotetramer equilibria.[17−19] We simulated a Job plot for a statistical distribution of homotetramers and heterotetramers and Job plots in which one of the heterotetramers is favored. These plots demonstrate how the relative stabilities of the tetramers affect the shapes of the curves. Figure 9 illustrates the resulting Job plots; the relative integrations of the species are plotted versus the mole fraction χ_B.

In the implementation by Collum and co-workers, the relative concentrations of the homotetramers and heterotetramers are calculated from equations based on a homotetramer-heterotetramer equilibrium model. The parameters $\phi_{N,n}$ are ascribed to
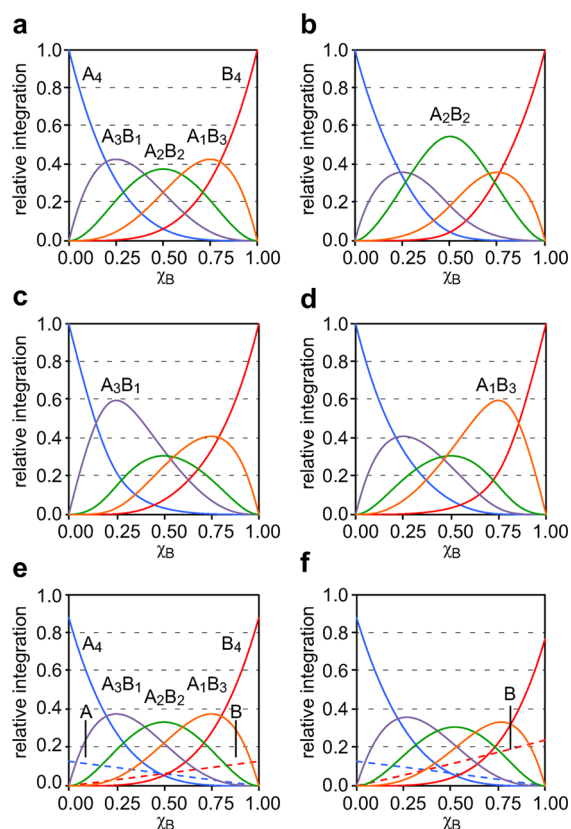
Figure 9. Simulated Job plots that show the relative integrations of the monomers, homotetramers, and heterotetramers versus the mole fraction of B, χ_B. (a) A statistical distribution of homotetramers and heterotetramers; $\phi_{4,4} = \phi_{4,3} = \phi_{4,2} = \phi_{4,1} = \phi_{4,0} = 1$. (b) A_2B_2 heterotetramer is favored; $\phi_{4,2} = 2$ and $\phi_{4,4} = \phi_{4,3} = \phi_{4,1} = \phi_{4,0} = 1$. (c) A_3B_1 heterotetramer is favored; $\phi_{4,3} = 2$ and $\phi_{4,4} = \phi_{4,2} = \phi_{4,1} = \phi_{4,0} = 1$. (d) A_1B_3 heterotetramer is favored; $\phi_{4,1} = 2$ and $\phi_{4,4} = \phi_{4,3} = \phi_{4,2} = \phi_{4,0} = 1$. (e) A statistical distribution of homotetramers and heterotetramers that also includes monomers; $\phi_{4,4} = \phi_{4,3} = \phi_{4,2} = \phi_{4,1} = \phi_{4,0} = 1$ and $\phi_{1,1} = \phi_{1,0} = 1$. (f) A statistical distribution of homotetramers and heterotetramers that also includes monomers, where the B monomer is favored $\phi_{4,4} = \phi_{4,3} = \phi_{4,2} = \phi_{4,1} = \phi_{4,0} = 1$, $\phi_{1,1} = 1$, and $\phi_{1,0} = 2$.

each of the homotetramers and heterotetramers in the equations, where the N and n are integers in which the value of N describes the oligomer size and the value of n describes the number of "A" subunits. The value of each $\phi_{N,n}$ reflects the relative stability of each homotetramer or heterotetramer. The parameters $\phi_{4,4}$, $\phi_{4,3}$, $\phi_{4,2}$, $\phi_{4,1}$, and $\phi_{4,0}$ describe the relative stabilities of A_4, A_3B_1, A_2B_2, A_1B_3, and B_4, respectively. When each tetramer is equally stable, all parameters are equal (e.g., $\phi_{4,4} = \phi_{4,3} = \phi_{4,2} = \phi_{4,1} = \phi_{4,0} = 1$) and a statistical distribution of homotetramers and heterotetramers forms.

The Job plot of a statistical distribution of homotetramers and heterotetramers is symmetrical, where the maximum of each curve reflects the tetramer stoichiometry. In the 1:1 mixture, the A_2B_2 heterotetramer predominates, with smaller fractions of the A_3B_1 and A_1B_3 heterotetramers in equal amounts, and with traces of the A_4 and B_4 homotetramers in equal amounts. In the 3:1 mixture, the A_3B_1 heterotetramer predominates, with smaller fractions of the A_4 homotetramer and A_2B_2 heterotetramer, and with traces of the A_1B_3 heterotetramer. Similarly, in the 1:3 mixture, the A_1B_3 heterotetramer predominates, with smaller fractions of the B_4 homotetramer and A_2B_2 heterotetramer, and

with traces of the A_3B_1 heterotetramer. Figure 9a illustrates the Job plot for a statistical distribution of homotetramers and heterotetramers.

The appearance of the Job plot changes if any of the tetramers are favored or disfavored. If the A_2B_2 tetramer is favored, the A_2B_2 curve shows a pronounced increase and the A_3B_1 and A_1B_3 curves diminish slightly (Figure 9b). If the A_3B_1 tetramer is favored, the A_3B_1 curve shows a pronounced increase and the A_2B_2 curve diminishes slightly (Figure 9c). If the A_1B_3 tetramer is favored, the A_1B_3 curve shows a pronounced increase and the A_2B_2 curve diminishes slightly (Figure 9d).

Analysis of the Job Plot. We modified the implementation by Collum and co-workers to accommodate the equilibrium of the monomers with the homotetramers and heterotetramers. In our implementation, the relative concentrations of the monomers, homotetramers, and heterotetramers are calculated from equations based on a monomer–homotetramer–heterotetramer equilibrium model. The parameters $\phi_{1,1}$ and $\phi_{1,0}$ reflect the relative stabilities of the monomers A and B. The Job plot of a statistical distribution of homotetramers and heterotetramers that also includes the monomers is similar to the Job plot without monomers, except that the fraction of each tetramer is slightly diminished (Figure 9e). If the equilibrium favors one of the two monomers, a greater fraction of that monomer forms (Figure 9f).

We analyzed the data from our Job's method experiment by nonlinear least-squares fitting of the model to the data. During the fit, the parameters $\phi_{4,3}$, $\phi_{4,2}$, $\phi_{4,1}$, $\phi_{4,0}$, $\phi_{1,1}$, and $\phi_{1,0}$ were allowed to vary, while the parameter $\phi_{4,4}$ remained fixed at 1. Figure 8 illustrates the Job plot with the fitted curves ($\phi_{4,4} = 1.00$, $\phi_{4,3} = 0.22$, $\phi_{4,2} = 0.67$, $\phi_{4,1} = 0.12$, $\phi_{4,0} = 0.12$, $\phi_{1,1} = 0.36$, $\phi_{1,0} = 2.20$).

The model fits the data well. The quality of the fit corroborates that peptides $[^{15}N]\mathbf{1a}$ and $[^{15}N]\mathbf{1b}$ form a mixture of homotetramers and heterotetramers. The appearance of the resulting plot does not resemble the statistical distribution shown in Figure 9e. The Job plot shows little or no preference for the A_2B_2 heterotetramer, but it does show suppression of the A_3B_1 and A_1B_3 heterotetramers.

The Job's method of continuous variation study and nonlinear least-squares fitting of the data establish that peptides $\mathbf{1a}$ and $\mathbf{1b}$ prefer to segregate within the heterotetramers. The suppression of the A_3B_1 and A_1B_3 heterotetramers shows that the A·B heterodimer subunit is disfavored and that heterotetramers containing an A·B heterodimer subunit are less stable. This finding explains why the A_2B_2 heterotetramer contains two homodimers rather than two heterodimers. Peptide $\mathbf{1a}$, which contains $A\beta_{17-23}$, prefers to pair with itself to form a hydrogen-bonded homodimer; peptide $\mathbf{1b}$, which contains $A\beta_{30-36}$, prefers to pair with itself to form a hydrogen-bonded homodimer.

Molecular Models of A_2B_2 Heterotetramers. We constructed energy-minimized models of A_2B_2 heterotetramers to help understand the preferential pairing of peptides $\mathbf{1a}$ and $\mathbf{1b}$ to form homodimers. By combining the monomer subunits of the models of the A_4 and B_4 homotetramers developed in the preceding paper,[6] and re-minimizing, we generated two models of the A_2B_2 heterotetramers: the A·A/B·B topological isomer that was observed, and the A·B/A·B topological isomer that was not. Figure 10 illustrates the resulting models of these two topological isomers.

The models show that the A_2B_2 heterotetramers can form sandwich-like structures that are similar to the homotetramers. Both topological isomers consist of two, four-stranded β-sheets
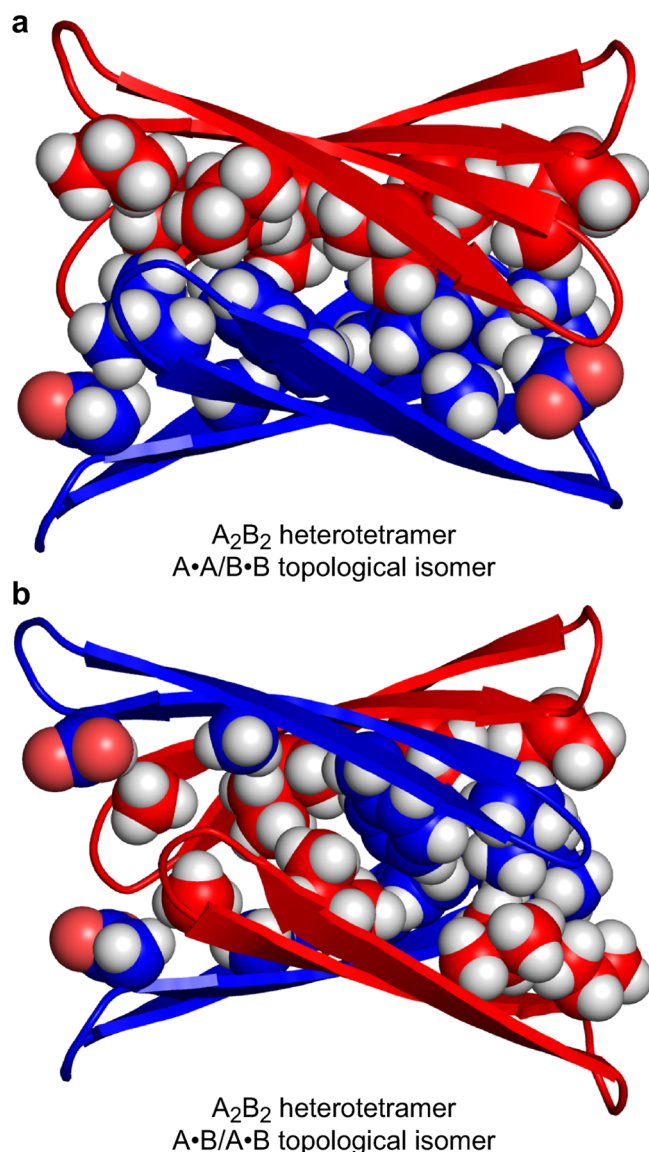
a

A$_2$B$_2$ heterotetramer
A·A/B·B topological isomer

b

A$_2$B$_2$ heterotetramer
A·B/A·B topological isomer

Figure 10. Molecular models of the topological isomers of the A$_2$B$_2$ heterotetramer of peptides **1a** and **1b**. (a) The A·A/B·B topological isomer. (b) The A·B/A·B topological isomer. Each model is a minimum-energy structure (local minimum) generated with Macro-Model using the MMFFs force field with GB/SA water solvation.

a

A·A homodimer of peptide **1a**

b

B·B homodimer of peptide **1b**
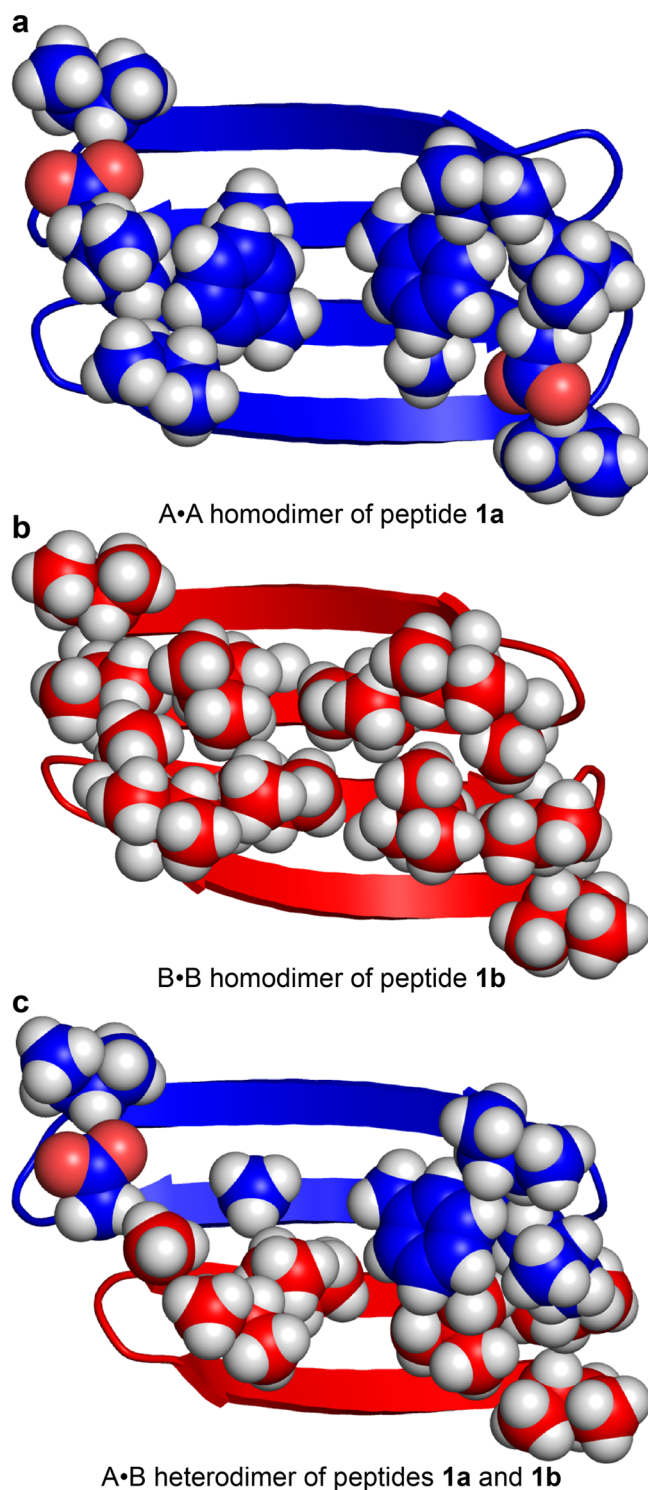
c

A·B heterodimer of peptides **1a** and **1b**

Figure 11. Molecular models of the homodimer and heterodimer subunits of the A$_2$B$_2$ heterotetramers of peptides **1a** and **1b**.

that laminate together through hydrophobic packing. The side chains of L$_{17}$, F$_{19}$, and A$_{21}$ from peptide **1a** and of A$_{30}$, I$_{32}$, L$_{34}$, and V$_{36}$ from peptide **1b** form hydrophobic surfaces that pack in the hydrophobic core of each heterotetramer. The interface between the A·A and B·B homodimers in the A·A/B·B topological isomer is uniformly packed. In contrast, the interface between the two A·B heterodimers in the A·B/A·B topological isomer is densely packed at one end and lightly packed at the other (Figure 10b).

The A·A homodimer of peptide **1a** exhibits a large hydrophobic surface, with intimate contacts between the side chains of L$_{17}$, F$_{19}$, and A$_{21}$. The large F$_{19}$ and small A$_{21}$ residues fit together well to help provide a uniformly packed surface (Figure 11a). The B·B homodimer of peptide **1b** also exhibits a large hydrophobic surface, with intimate contacts between the side chains of A$_{30}$, I$_{32}$, L$_{34}$, and V$_{36}$. These residues also provide a uniformly packed surface (Figure 11b). The A·B heterodimer

exhibits a hydrophobic surface with intimate contacts between the side chains of L$_{17}$, F$_{19}$, and A$_{21}$ from peptide **1a** and the side chains of I$_{32}$, L$_{34}$, and V$_{36}$ from peptide **1b**. The side chains do not pack uniformly, but rather the side chains pack densely at one end of the dimer and pack lightly at the other (Figure 11c).

These molecular models suggest that differences between the homodimers and heterodimers formed by peptides **1a** and **1b** dictate the observed differences in the A$_2$B$_2$ heterotetramer stability. The uniform packing of the A·A and B·B homodimers

appears to drive the formation of the observed A_2B_2 heterotetramer. The non-uniform packing of the A·B heterodimer appears to suppress the formation of the A_3B_1 and A_1B_3 heterotetramers, and also the alternative topological isomer of the A_2B_2 heterotetramer.

CONCLUSION

In framing the question behind these studies, we set out to determine whether peptides derived from the central and C-terminal regions of $A\beta$ prefer to coassemble or to segregate. We found that the answer is more nuanced, at least in the context of the model system provided by peptides **1**. Peptides **1a** and **1b** can coassemble, but the resulting heterotetramers reflect a preference to segregate within the dimer subunits. The heterotetramers comprising heterodimers are disfavored, while the heterotetramers comprising homodimers are not. These findings recapitulate the segregation within $A\beta_{1-40}$ fibrils, in which the central region assembles to form a hydrogen-bonded β-sheet and the C-terminal region assembles to form a hydrogen-bonded β-sheet.[3] The two β-sheets coassemble through hydrophobic contacts.

^{15}N-Isotopic labeling, ^{1}H,^{15}N NMR spectroscopy, and Job's method of continuous variation proved essential in these studies. Incorporation of a single ^{15}N-isotopic label provided a sensitive and non-perturbing spectroscopic probe. ^{15}N-Labeled peptides are readily prepared from commercially available ^{15}N-labeled amino acids using solid-phase peptide synthesis. ^{1}H,^{15}N HSQC facilitated identification of the monomers, homotetramers, and heterotetramers. Job's method of continuous variation assigned the resonances of each monomer and tetramer and established the relative stability of the tetramers. ^{15}N-Edited NOESY established the identity of the topological isomer of the A_2B_2 heterotetramer.

These techniques, which proved useful for elucidating the assembly and coassembly of β-sheet peptides, should also be valuable in broader contexts. Peptide and protein assemblies occur widely in coiled coils, helix bundles, and collagen helices, as well as in amyloid oligomers and other β-sheet supramolecular assemblies. We envision that ^{15}N-isotopic labeling in conjunction with ^{1}H,^{15}N NMR spectroscopy and Job's method will also be valuable for studying these assemblies.

ASSOCIATED CONTENT

Ⓢ Supporting Information

The Supporting Information is available free of charge on the ACS Publications website at DOI: 10.1021/jacs.6b06001.

> Figures S1−S5, showing NMR spectroscopic data; materials and methods; mathematical derivation for the monomer−homotetramer−heterotetramer equilibrium model; and procedures for nonlinear least-squares fitting of the Job plot data (PDF)

AUTHOR INFORMATION

Corresponding Author

*jsnowick@uci.edu

Notes

The authors declare no competing financial interest.

ACKNOWLEDGMENTS

REFERENCES

(1) (a) Näslund, J.; Haroutunian, V.; Mohs, R.; Davis, K. L.; Davies, P.; Greengard, P.; Buxbaum, J. D. *JAMA* **2000**, *283*, 1571−1577. (b) Haass, C.; Selkoe, D. J. *Nat. Rev. Mol. Cell Biol.* **2007**, *8*, 101−112. (c) Querfurth, H. W.; LaFerla, F. M. *N. Engl. J. Med.* **2010**, *362*, 329−344. (d) Knowles, T. P.; Vendruscolo, M.; Dobson, C. M. *Nat. Rev. Mol. Cell Biol.* **2014**, *15*, 384−396.

(2) Liu, R.; McAllister, C.; Lyubchenko, Y.; Sierks, M. R. *J. Neurosci. Res.* **2004**, *75*, 162−171.

(3) (a) Petkova, A. T.; Ishii, Y.; Balbach, J. J.; Antzutkin, O. N.; Leapman, R. D.; Delaglio, F.; Tycko, R. *Proc. Natl. Acad. Sci. U. S. A.* **2002**, *99*, 16742−16747. (b) Paravastu, A. K.; Leapman, R. D.; Yau, W.-M.; Tycko, R. *Proc. Natl. Acad. Sci. U. S. A.* **2008**, *105*, 18349−18354. (c) Tycko, R.; Wickner, R. B. *Acc. Chem. Res.* **2013**, *46*, 1487−1496. (d) Lu, J.-X.; Qiang, W.; Yau, W.-M.; Schwieters, C. D.; Meredith, S. C.; Tycko, R. *Cell* **2013**, *154*, 1257−1268.

(4) The fibrils formed by $A\beta_{1-42}$ adopt a more compact structure: (a) Xiao, Y.; Ma, B.; McElheny, D.; Parthasarathy, S.; Long, F.; Hoshi, M.; Nussinov, R.; Ishii, Y. *Nat. Struct. Mol. Biol.* **2015**, *22*, 499−505. (b) Walti, M. A.; Ravotti, F.; Arai, H.; Glabe, C. G.; Wall, J. S.; Bockmann, A.; Guntert, P.; Meier, B. H.; Riek, R. *Proc. Natl. Acad. Sci. U. S. A.* **2016**, *113*, E4976−E4984. (c) Colvin, M. T.; Silvers, R.; Ni, Q. Z.; Can, T. V.; Sergeyev, I.; Rosay, M.; Donovan, K. J.; Michael, B.; Wall, J.; Linse, S.; Griffin, R. G. *J. Am. Chem. Soc.* **2016**, *138*, 9663−9674.

(5) (a) Hoyer, W.; Gronwall, C.; Jonsson, A.; Stahl, S.; Hard, T. *Proc. Natl. Acad. Sci. U. S. A.* **2008**, *105*, 5099−5104. (b) Cerf, E.; Sarroukh, R.; Tamamizu-Kato, S.; Breydo, L.; Derclaye, S.; Dufrene, Y. F.; Narayanaswami, V.; Goormaghtigh, E.; Ruysschaert, J. M.; Raussens, V. *Biochem. J.* **2009**, *421*, 415−423. (c) Yu, L.; Edalji, R.; Harlan, J. E.; Holzman, T. F.; Lopez, A. P.; Labkovsky, B.; Hillen, H.; Barghorn, S.; Ebert, U.; Richardson, P. L.; Miesbauer, L.; Solomon, L.; Bartley, D.; Walter, K.; Johnson, R. W.; Hajduk, P. J.; Olejniczak, E. T. *Biochemistry* **2009**, *48*, 1870−1877. (d) Sandberg, A.; Luheshi, L. M.; Söllvander, S.; Pereira de Barros, T.; Macao, B.; Knowles, T. P. J.; Biverstål, H.; Lendel, C.; Ekholm-Petterson, F.; Dubnovitsky, A.; Lannfelt, L.; Dobson, C. M.; Härd, T. *Proc. Natl. Acad. Sci. U. S. A.* **2010**, *107*, 15595−15600. (e) Lendel, C.; Bjerring, M.; Dubnovitsky, A.; Kelly, R. T.; Filippov, A.; Antzutkin, O. N.; Nielsen, N. C.; Hard, T. *Angew. Chem., Int. Ed.* **2014**, *53*, 12756−12760. (f) Spencer, R. K.; Li, H.; Nowick, J. S. *J. Am. Chem. Soc.* **2014**, *136*, 5595−5598. (g) Kreutzer, A. G.; Hamza, I. L.; Spencer, R. K.; Nowick, J. S. *J. Am. Chem. Soc.* **2016**, *138*, 4634−4642.

(6) Truex, N. L.; Wang, Y.; Nowick, J. S. *J. Am. Chem. Soc.* **2016**, DOI: 10.1021/jacs.6b06000.

(7) (a) Cheng, P. N.; Liu, C.; Zhao, M.; Eisenberg, D.; Nowick, J. S. *Nat. Chem.* **2012**, *4*, 927−933. (b) Liu, C.; Zhao, M.; Jiang, L.; Cheng, P. N.; Park, J.; Sawaya, M. R.; Pensalfini, A.; Gou, D.; Berk, A. J.; Glabe, C. G.; Nowick, J.; Eisenberg, D. *Proc. Natl. Acad. Sci. U. S. A.* **2012**, *109*, 20913−20918. (c) Buchanan, L. E.; Dunkelberger, E. B.; Tran, H. Q.; Cheng, P. N.; Chiu, C. C.; Cao, P.; Raleigh, D. P.; de Pablo, J. J.; Nowick, J. S.; Zanni, M. T. *Proc. Natl. Acad. Sci. U. S. A.* **2013**, *110*, 19285−19290.

(8) Nowick, J. S.; Chung, D. M.; Maitra, K.; Maitra, S.; Stigers, K. D.; Sun, Y. *J. Am. Chem. Soc.* **2000**, *122*, 7654−7661.

(9) (a) Nowick, J. S.; Brower, J. O. *J. Am. Chem. Soc.* **2003**, *125*, 876−877. (b) Woods, R. J.; Brower, J. O.; Castellanos, E.; Hashemzadeh, M.; Khakshoor, O.; Russu, W. A.; Nowick, J. S. *J. Am. Chem. Soc.* **2007**, *129*, 2548−2558.

(10) For some related studies of peptide and protein coassembly, see: (a) Hammarstrom, P.; Schneider, F.; Kelly, J. W. *Science* **2001**, *293*, 2459−2462. (b) Schnarr, N. A.; Kennan, A. J. *J. Am. Chem. Soc.* **2002**, *124*, 9779−9783. (c) Hadley, E. B.; Testa, O. D.; Woolfson, D. N.; Gellman, S. H. *Proc. Natl. Acad. Sci. U. S. A.* **2008**, *105*, 530−535. (d) Xu, F.; Zahid, S.; Silva, T.; Nanda, V. *J. Am. Chem. Soc.* **2011**, *133*, 15260−15263. (e) Fallas, J. A.; Hartgerink, J. D. *Nat. Commun.* **2012**, *3*, 1087. (f) Thomas, F.; Boyle, A. L.; Burton, A. J.; Woolfson, D. N. *J. Am. Chem. Soc.* **2013**, *135*, 5161−5166. (g) Negron, C.; Keating, A. E. *J. Am. Chem. Soc.* **2014**, *136*, 16544−16556.

(11) (a) Khakshoor, O.; Demeler, B.; Nowick, J. S. *J. Am. Chem. Soc.* **2007**, *129*, 5558−5569. (b) Pham, J. D.; Demeler, B.; Nowick, J. S. *J. Am. Chem. Soc.* **2014**, *136*, 5432−5442. (c) Pham, J. D.; Spencer, R. K.; Chen, K. H.; Nowick, J. S. *J. Am. Chem. Soc.* **2014**, *136*, 12682−12690.

(12) We used ^1H NMR TOCSY to assign residues associated with these NOEs (Figures S1 and S2).

(13) The ^1H NMR NOESY spectrum of the 1:1 mixture of peptides **1a** and **1b** shows additional NOEs associated with the stacking of the two homodimers to form a sandwich-like tetramer. The spectrum shows NOEs between the F_{19} aromatic protons of peptide **1a** and the I_{32} and L_{34} side-chain protons of peptide **1b** (Figure S4a). The spectrum also shows NOEs between the A_{21} side-chain protons of peptide **1a** and the I_{32} side-chain protons of peptide **1b** (Figure S4b). Figure S5 illustrates the stacking of the A·A and B·B homodimers of peptides **1a** and **1b** consistent with these NOEs.

(14) Job, P. *Ann. Chim. Fr.* **1928**, *9*, 113−203.

(15) (a) Ramanathan, P. S. *J. Inorg. Nucl. Chem.* **1973**, *35*, 3358−3360. (b) Ingham, K. C. *Anal. Biochem.* **1975**, *68*, 660−663. (c) Huang, C. Y. *Methods Enzymol.* **1982**, *87*, 509. (d) Gil, V. M. S.; Oliveira, N. C. *J. Chem. Educ.* **1990**, *67*, 473−478. (e) Facchiano, A.; Ragone, R. *Anal. Biochem.* **2003**, *313*, 170−172. (f) Renny, J. S.; Tomasevich, L. L.; Tallmadge, E. H.; Collum, D. B. *Angew. Chem., Int. Ed.* **2013**, *52*, 11998−12013.

(16) The 8.0 mM total concentration was chosen to favor tetramers in the mixtures of peptides [^{15}N]**1a** and [^{15}N]**1b**.

(17) (a) McNeil, A. J.; Toombes, G. E.; Chandramouli, S. V.; Vanasse, B. J.; Ayers, T. A.; O'Brien, M. K.; Lobkovsky, E.; Gruner, S. M.; Marohn, J. A.; Collum, D. B. *J. Am. Chem. Soc.* **2004**, *126*, 5938−5939. (b) McNeil, A. J.; Toombes, G. E.; Gruner, S. M.; Lobkovsky, E.; Collum, D. B.; Chandramouli, S. V.; Vanasse, B. J.; Ayers, T. A. *J. Am. Chem. Soc.* **2004**, *126*, 16559−16568. (c) Liou, L. R.; McNeil, A. J.; Ramirez, A.; Toombes, G. E.; Gruver, J. M.; Collum, D. B. *J. Am. Chem. Soc.* **2008**, *130*, 4859−4868.

(18) Widom, B. *Statistical Mechanics: A Concise Introduction for Chemists*; Cambridge University Press: New York, 2002.

(19) Additional references on quantitative treatment of data from Job's method of continuous variation: (a) Likussar, W.; Boltz, D. F. *Anal. Chem.* **1971**, *43*, 1265−1272. (b) Bruneau, E.; Lavabre, D.; Levy, G.; Micheau, J. C. *J. Chem. Educ.* **1992**, *69*, 833−837. (c) Hirose, K. *J. Inclusion Phenom. Mol. Recognit. Chem.* **2001**, *39*, 193−209. (d) Olson, E. J.; Bühlmann, P. *J. Org. Chem.* **2011**, *76*, 8406−8412. (e) Olson, E. J.; Bühlmann, P. *J. Org. Chem.* **2014**, *79*, 830−830. (f) Hirose, K. In *Analytical Methods in Supramolecular Chemistry*, 2nd ed.; Schalley, C. A., Ed.; Wiley-VCH: Weinheim, 2012; pp 27−66.